Citation: Molecular Therapy—Nucleic Acids (2013) 2, e136; doi:10.1038/mtna.2013.65

www.nature.com/mtna

Lipid Nanoparticle Delivery of siRNA to Silence Neuronal Gene Expression in the Brain

Ravi L Rungta[1], Hyun B Choi[1], Paulo JC Lin[2], Rebecca WY Ko[1], Donovan Ashby[1], Jay Nair[3], Muthiah Manoharan[3], Pieter R Cullis[2] and Brian A MacVicar[1]

Manipulation of gene expression in the brain is fundamental for understanding the function of proteins involved in neuronal processes. In this article, we show a method for using small interfering RNA (siRNA) in lipid nanoparticles (LNPs) to efficiently silence neuronal gene expression in cell culture and in the brain *in vivo* through intracranial injection. We show that neurons accumulate these LNPs in an apolipoprotein E–dependent fashion, resulting in very efficient uptake in cell culture (100%) with little apparent toxicity. *In vivo*, intracortical or intracerebroventricular (ICV) siRNA-LNP injections resulted in knockdown of target genes either in discrete regions around the injection site or in more widespread areas following ICV injections with no apparent toxicity or immune reactions from the LNPs. Effective targeted knockdown was demonstrated by showing that intracortical delivery of siRNA against GRIN1 (encoding GluN1 subunit of the NMDA receptor (NMDAR)) selectively reduced synaptic NMDAR currents *in vivo* as compared with synaptic AMPA receptor currents. Therefore, LNP delivery of siRNA rapidly manipulates expression of proteins involved in neuronal processes *in vivo*, possibly enabling the development of gene therapies for neurological disorders.

Molecular Therapy—Nucleic Acids (2013) **2**, e136; doi:10.1038/mtna.2013.65; published online 3 December 2013
Subject Category: siRNAs, shRNAs, and miRNAs Nanoparticles

Introduction

Since the discovery that RNA interference is mediated by double-stranded RNA,[1] the use of small interfering RNA (siRNA) to silence specific genes has become a powerful method for manipulating gene expression *in vitro* and, increasingly, *in vivo*. However, issues concerning the delivery of siRNA into neurons both *in vitro* and *in vivo* limit the widespread use of siRNA in neuroscience research in mammals. Viral delivery of short hairpin RNA (shRNA) has been used successfully *in vivo* (e.g., ref. 2) to knock down selected targets, but the time and expense of packaging shRNA into high-titer viruses, as well as the toxicological and immunological problems associated with viral vectors, must be considered. In cell culture, the use of siRNA approaches for silencing genes in neurons remains limited due to the low transfection levels and the toxicity observed with techniques that use lipofectamine. Transgenic approaches to modulate central nervous system gene expression are time consuming and costly. Antisense oligonucleotides (ASOs) can be effective when their stabilized forms are injected into the brain, but large quantities of ASOs need to be injected for effective uptake. The development of alternative delivery methods to facilitate the use of siRNA to manipulate gene expression in the mammalian central nervous system would be of great value to neuroscientists and would accelerate progress in our understanding of brain function.

Lipid nanoparticles (LNPs) are currently the leading delivery systems for enabling the therapeutic potential of siRNA in peripheral cells.[3,4] LNP-siRNA systems containing optimized cationic lipids can silence therapeutically relevant genes in a variety of tissues (particularly liver)[5–7] following intravenous (IV) injection in animal models. Positive clinical trial results using these LNPs have been reported for the treatment of cardiovascular disease, certain forms of amyloidosis, and other disorders (http://www.alnylam.com/Programs-and-Pipeline/Alnylam-5x15/index.php). However, the efficacy of LNP approaches for delivering siRNA to neurons in the central nervous system is unknown. Due to the inability of LNP systems to cross the blood–brain barrier, the potency of these systems for silencing genes in brain tissue has not been investigated. In this article, we report the conditions under which LNP delivery of siRNA is a remarkably efficient method for silencing neuronal gene expression in both primary neuronal culture and following intracranial injection *in vivo*.

Results

Encapsulation of siRNA in LNPs

LNPs were prepared by mixing appropriate volumes of lipid mixture in ethanol with an aqueous phase containing siRNA duplexes using a microfluidic micromixer (**Figure 1a**) as described elsewhere.[8] The lipid composition used was 3-(dimethylamino)propyl(12Z,15Z)-3-[(9Z,12Z)-octadeca-9,12-dien-1-yl]henicosa-12,15-dienoate (DMAP-BLP) (structure shown in **Figure 1b**)/distearoylphosphatidylcholine (DSPC)/cholesterol/PEG-DMG in the molar percentage ratios 50/10/37.5/1.5. The LNPs also contained 1 mol% of the fluorescently labeled lipids $DiOC_{18}$ or $DiIC_{18}$ to monitor LNP uptake. Previous work has shown that LNP systems with this lipid composition can silence target genes in hepatocytes following IV injection at dose levels as low as 0.01 mg siRNA/kg body weight[8,9] in an apolipoprotein E (ApoE)–dependent

The first three authors contributed equally to this work.

[1]Brain Research Centre, Department of Psychiatry, University of British Columbia, British Columbia, Canada; [2]Department of Biochemistry and Molecular Biology, University of British Columbia, British Columbia, Canada; [3]Alnylam Pharmaceuticals, Cambridge, Massachusetts, USA. Correspondence: Brian A MacVicar, Brain Research Centre, Department of Psychiatry, University of British Columbia, 2211 Wesbrook Mall, Vancouver, British Columbia V6T 2B5, Canada. E-mail: bmacvicar@brain.ubc.ca
Received 26 July 2013; accepted 23 September 2013; advance online publication 3 December 2013. doi:10.1038/mtna.2013.65

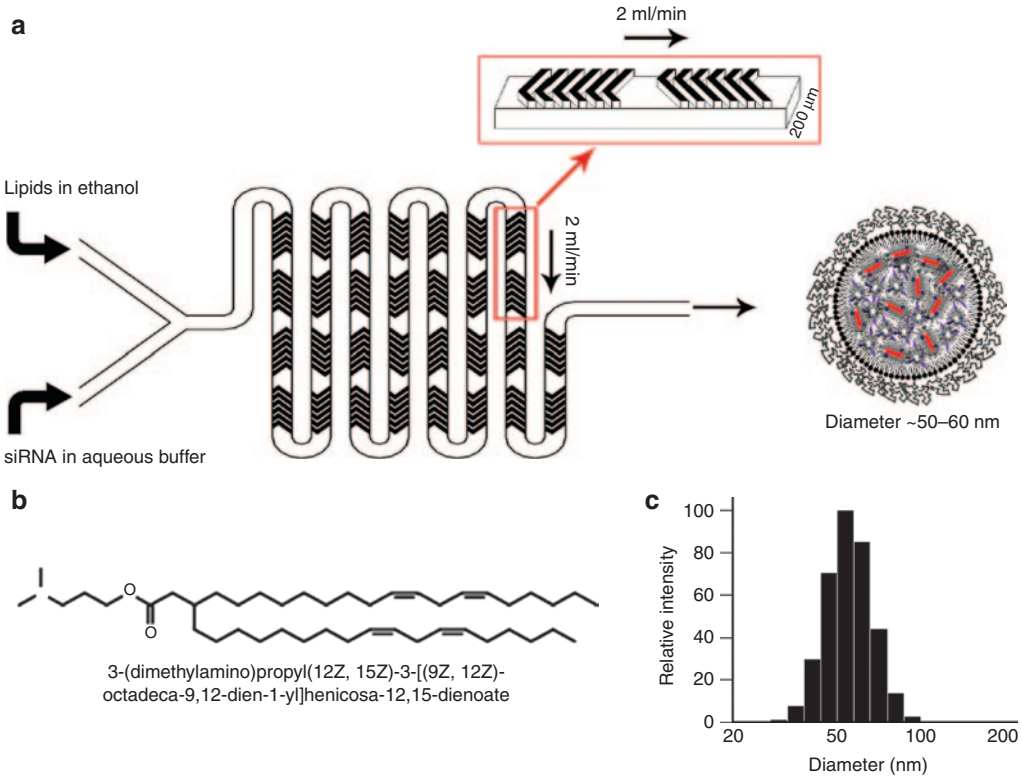

Figure 1 Schematic of LNP-siRNA formulation process employing the staggered herringbone micromixer. (**a**) The lipid mixture in ethanol and siRNA in aqueous solution are pumped separately into the two inlets of the microfluidic mixing device using a syringe pump with a total flow rate of 2 ml/minute. Herringbone structures induce chaotic advection of the laminar streams causing rapid mixing of the ethanol and aqueous phases and correspondingly rapid increases in the polarity experienced by the lipid solution. At a critical polarity the precipitates form as LNPs. Dimensions of the mixing channel were 200×79 µm, and the herringbone structures were 31 µm high and 50 µm thick. Modified from ref. 8. (**b**) Chemical structure of ionizable cationic lipid—3-(dimethylamino)propyl(12Z,15Z)-3-[(9Z,12Z)-octadeca-9,12-dien-1-yl]henicosa-12,15-dienoate (DMAP-BLP). (**c**) Representative size distribution of LNPs (LNP PTEN-siRNA) analyzed in number mode using the NICOMP 370 Submicron Particle Sizer. LNP, lipid nanoparticle; siRNA, small interfering RNA.

fashion.[10] The LNP phosphatase and tensin homolog 1 (PTEN)-siRNA systems produced had a diameter 55±11 nm (size distribution is shown in **Figure 1c**). The sizes of the other LNP-siRNA systems are listed in **Supplementary Table S1**. No further optimization was done to increase the efficiency of LNP-siRNA systems in this study.

LNP-mediated neuronal gene silencing *in vitro*

To test whether LNPs are taken up by neurons, cultured neurons were incubated with siRNA-containing LNPs at a final concentration of 246 nmol/l (3.3 µg siRNA/ml). For LNPs of 55 nm diameter at a siRNA-to-lipid ratio of 0.056 (mg/µmol), this represents ~5.6×10^{11} LNPs/ml. We used a culture system containing pure hippocampal neurons on a coverslip with astrocytes on a separate feeder layer (**Figure 2a**).[11] Surprisingly, we found that 100% of neurons in the culture dish had taken up LNPs following incubation for 24 hours, as indicated by discrete punctate DiI fluorescence within neurons (**Figure 2b**). DiI-labeled intracellular puncta were observed both in live cultured neurons and in neurons after cultures were fixed. The punctate staining pattern of DiI indicates LNPs located in endosomes and lysosomes.[6] LNPs were nontoxic at the concentrations used, with no observable differences in cell death relative to controls measured either by comparing nuclear morphology or by lactate dehydrogenase (LDH) release (**Figure 2c**). As a positive control, cultures treated with 1% Triton X-100 showed a large increase in LDH release (90.21±0.62%).

We next tested whether the LNP-mediated delivery of siRNA to neurons effectively silenced gene expression by using Western blots to examine changes in protein expression encoded by the corresponding target gene. We first tested LNP delivery of siRNA against PTEN, a protein highly expressed in pyramidal neurons.[12] Incubation of primary rat neuronal cultures with LNPs containing PTEN siRNA (246 nmol/l) for 48 hours resulted in robust knockdown of PTEN protein indicated by Western blot (PTEN/β-actin reduced by 80% compared with control; $P < 0.001$, **Figure 2d**). Of note, in control experiments, incubation of cultures with LNPs containing siRNA against luciferase (luc), which is not found in the mammalian genome, had no effect on levels of PTEN protein (**Figure 2d**). In addition, neurons treated with nonencapsulated PTEN siRNA (246 nmol/l) showed no significant change in PTEN/β-actin compared with control (**Figure 2e**). To determine the efficiency of these LNP-siRNA systems, we performed a dose response curve and found that even concentrations as low as 0.7 nmol/l resulted in robust protein knockdown (PTEN/β-actin reduced by 59% compared with control; $P < 0.001$, **Figure 2e**). These results indicate that LNPs are much more efficient and less toxic than current methods used to deliver siRNA to cultured neurons

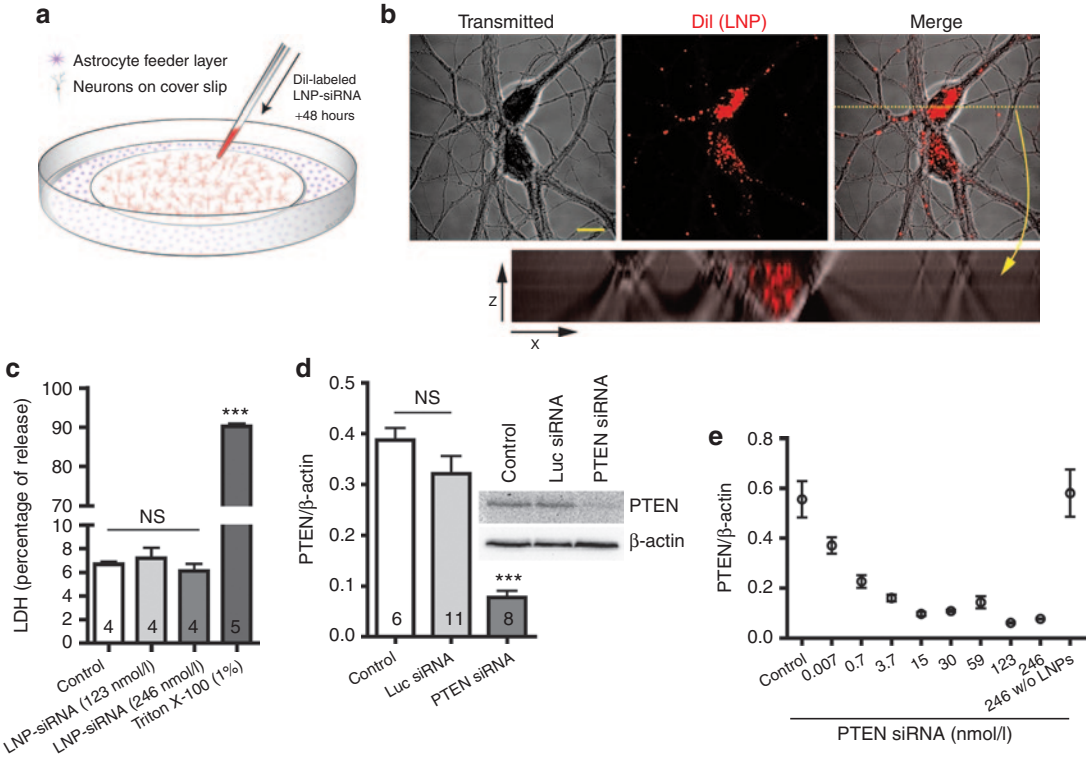

Figure 2 LNP-siRNA systems mediate knockdown of target gene in neuron cultures. (**a**) Pure neuron cultures on a coverslip in a petri dish with a separate astrocyte feeder layer. LNP-siRNA was added directly to the media. (**b**) DiI fluorescence (red) shows that LNPs are found in the cytoplasm of neurons. Bottom: cross-sectional analysis of an image stack of fluorescence and transmitted IR images revealed that that DiI puncta were found within the boundaries of the cell membrane. scale: 15 μm. (**c**) Quantification of LDH release revealed that LNPs were not toxic at concentrations used. (**d**) Western blots reveal LNP-PTEN siRNA resulted in knockdown of PTEN protein compared with luc siRNA-LNP control and nontreated cultures. (**e**) Dose response of LNP-siRNA concentration versus PTEN knockdown, last column shows that nonencapsulated siRNA did not result in protein knockdown. In all figures, experimental values are the mean and SEM. LDH, lactate dehydrogenase; LNP, lipid nanoparticle; NS, not significant; siRNA, small interfering RNA.

such as electroporation, calcium phosphate, or lipofection, which usually result in transfection rates of 1–10%.[13] Higher transfection rates have been reported on optimization, but generally at the expense of cell toxicity.[13]

In hepatocytes *in vivo*, LNP uptake is facilitated by adsorption of ApoE to the LNPs,[10] which can then be recognized by scavenging receptors and low-density lipoprotein receptors (LDLRs) on the hepatocyte surface. Because ApoE is the dominant lipoprotein in the brain, we tested whether ApoE facilitates uptake of LNPs by neurons in cell culture. ApoE is produced mainly by astrocytes and delivers cholesterol and other essential lipids to neurons via binding to members of the LDLR family followed by endocytosis.[14,15] To directly test whether the ApoE could facilitate LNP uptake into neurons, we transferred the neurons to media that had not been in contact with astrocytes and applied LNPs (246 nmol/l) with or without exogenous ApoE4 (10 μg/ml) (**Figure 3a**). After 1 hour, we noticed rapid uptake of DiI-labeled LNPs in the presence of exogenous ApoE, compared with neurons incubated without ApoE4 (**Figure 3a**,**b**). Furthermore, we tested the dose dependence of ApoE versus LNP uptake by measuring the total DiI fluorescence from ruptured cells 1 hour after treatment. We found that LNP uptake reached saturation at ~5 μg ApoE/ml (**Figure 3c**), in line with measurements from human cerebrospinal fluid (CSF) *in vivo* of 9.09 μg/ml.[16] These results suggest that the efficient LNP uptake by neurons is facilitated by association with ApoE and subsequent endocytosis into neurons via an ApoE receptor.

LNP-mediated neuronal gene silencing *in vivo*

The gene silencing potency of LNP-siRNA formulations was tested *in vivo* by direct injection into the cortex. In these experiments, a single injection of LNPs (500 nl at 5 mg/ml siRNA/10 minutes) was administered directly into the somatosensory cortex (**Figure 4a**), and the distribution of DiI-labeled LNPs and the impact on gene expression were monitored subsequently. These LNPs had an average diameter of 50–60 nm (**Figure 1c**), small enough to diffuse through the extracellular space of the brain.[17] To first test whether neurons *in vivo* accumulated LNPs, acute cortical slices were made from injected rats 5 days following injection and monitored for DiI positive neurons. Astrocytes *in vivo* produce and secrete ApoE;[15] therefore, no additional ApoE was added to injected LNPs. We consistently found robust DiI staining localized to neurons within a radius of ~800 μm from the injection site (**Figure 4b**). The neurons were visualized using a live cell fluorescent assay by loading the cells with an acetoxymethyl (AM) form of a fluorescent Na^+ dye, CoroNa-AM that is only retained in live cells.[18] Consistent with the *in vitro* cell culture results, a single injection of LNP-PTEN siRNA resulted in knockdown of PTEN

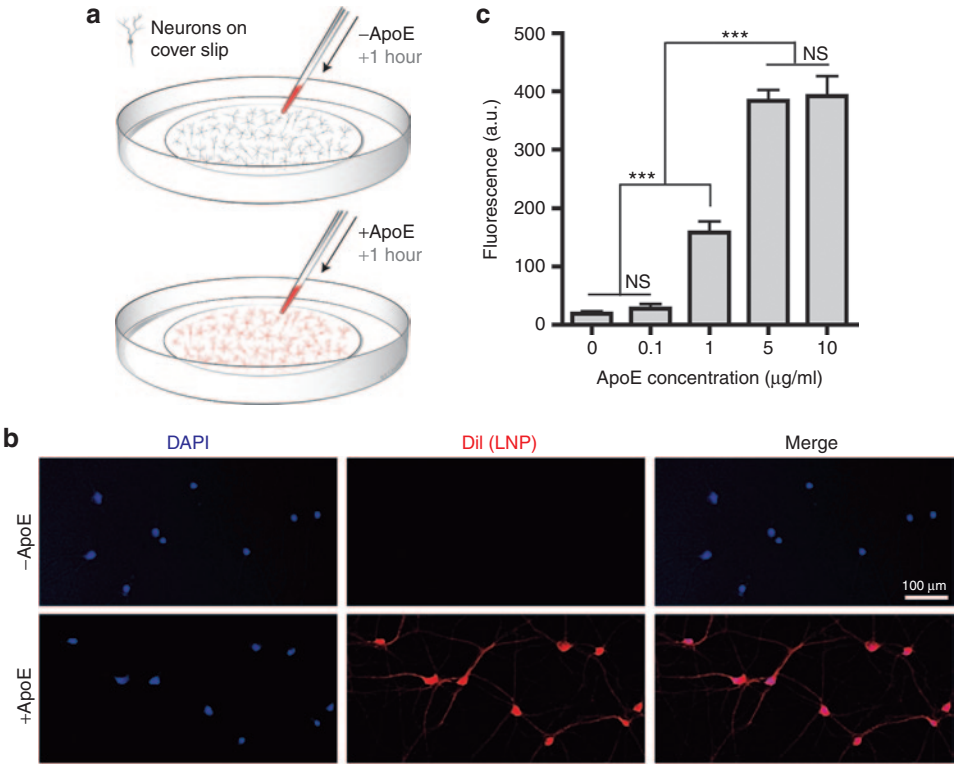

Figure 3 Lipid nanoparticles (LNPs) are taken up by neurons in an apolipoprotein E (ApoE)–dependent manner. (**a**,**b**) In the absence of astrocytes, addition of ApoE facilitated the uptake of LNPs by neurons shown by an increase in DiI fluorescence. Treatment: 1 hour LNP-siRNA ± ApoE. Scale: 100 μm. (**c**) Dose dependence of LNP uptake versus ApoE concentration measured as DiI fluorescence. In all figures, experimental values are the mean and SEM. ***$P < 0.001$. DAPI, 4′,6-diamidino-2-phenylindole; NS, not significant; siRNA, small interfering RNA.

protein measured using Western blots (PTEN to β-actin ratios reduced by 72 and 69% compared with noninjected or luc siRNA–injected controls, respectively, $P < 0.001$, **Figure 4c**,**d**). Luc siRNA–injected tissue was not significantly different from noninjected controls (**Figure 4c**,**d**). In addition, to test for toxicity of LNPs *in vivo*, we loaded cells with the vital dye calcein-AM, which is fluorescent only when cleaved by endogenous esterases present in live cells and compared cell density in LNP-injected rats and noninjected rats. In luc siRNA-LNP–injected rats, we observed no significant difference in cell density 200–500 μm from the injection tract compared with control (**Figure 4e**). This is a region with robust LNP uptake and gene knockdown but not damaged from the injection needle itself, suggesting that LNPs themselves are nontoxic *in vivo*. These results demonstrate that when administered directly into the brain, LNPs are capable of diffusing through the extracellular milieu to deliver siRNA to neurons and induce gene silencing at sites distant from the site of injection.

Although clinical studies suggest that IV delivery of LNP-siRNAs is rarely immunogenic, the immunostimulatory effects of LNPs on brain tissue have not yet been examined. To test whether LNP-siRNAs caused any immunostimulatory effects in the brain, we directly incubated acute cortical/hippocampal brain slices in LNP-siRNA and measured immune responses using tumor necrosis factor-α (TNF-α) enzyme-linked immunosorbent assay (ELISA). TNF-α is a proinflammatory cytokine, which is released when immune responses occur in the brain. The results suggest that there was no immunostimulatory effect when luc siRNA-LNPs (246 nmol/l) were applied to brain slices. TNF-α levels in the luc siRNA-LNP–treated group were not significantly different from the control group (**Figure 4f**, $P > 0.05$). As a positive control, lipopolysaccharide (40 μg/ml) was applied to the slices, which induced a significant increase of TNF-α compared with control and luc siRNA-LNP groups (**Figure 4f**, $P < 0.05$). In addition, TNF-α levels were not significantly increased in siRNA-LNP–positive tissue following direct injection *in vivo* (**Figure 4g**, $P > 0.05$). These data suggest that LNPs themselves do not cause immunostimulatory responses in the brain.

Time course and distance analysis of PTEN knockdown *in vivo*

We next determined how far from the injection site was gene silencing effectively induced, as well as the time course of the LNP-mediated PTEN knockdown. To characterize the distance profile of the knockdown, we used a combination of immunohistochemistry and Western blot analysis on tissue taken at different distances away from the injection tract. Immunostaining of fixed tissue taken from rats 5 days following a single injection of PTEN siRNA-LNPs revealed clear loss of PTEN staining in neurons less than 1 mm from the injection site, compared with higher levels of PTEN staining at distances further away (**Figure 5a**). The montage in **Figure 5a** shows a sectioning plane where the asterisk indicates the region 400 μm posterior to the injection tract. The pattern of decreased immunofluorescence showed a good

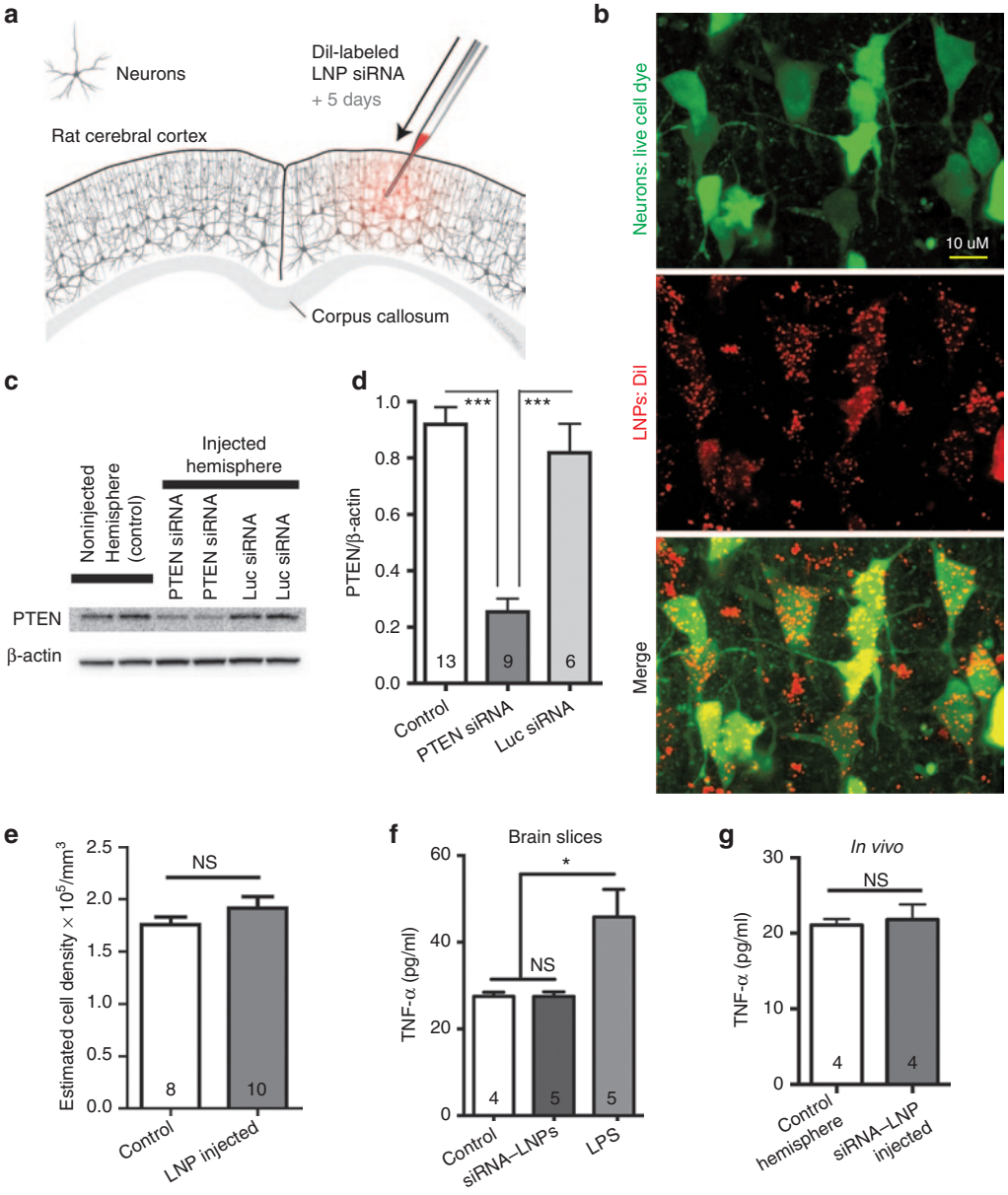

Figure 4 LNP-siRNA systems mediate knockdown of target gene *in vivo*. (**a**) LNP-siRNA was injected directly into the somatosensory cortex using a glass micropipette. (**b**) Imaging of acute brain slices 5 days following a single injection of LNP-siRNA revealed that live neurons (AM dye) had taken up fluorescent LNPs (DiI). (**c**,**d**) Western blots revealed that injection of LNP-PTEN siRNA resulted in knockdown of PTEN protein compared with tissue from the noninjected hemisphere and luc siRNA-LNP–injected rats. Tissue was dissected within 1 mm from the site of injection after 5 days. (**e**) Analysis of the density of live cells stained with the vital dye calcein-AM showed that there was no indication of toxicity or cell loss with LNP uptake *in vivo* (200–500 μm from injection). (**f**) TNF-α ELISA measurement from acute brain slices treated with luc siRNA-LNPs shows lack of an immunostimulatory response to LNPs in brain tissue. Positive control, LPS-treated slices show increase in TNF-α. (**g**) TNF-α ELISA measurements taken from LNP-positive tissue (~100–500 μm from injection) were not significantly different from the LNP-negative noninjected hemisphere. Measurements were normalized to 0.5 mg of protein. $^*P < 0.05$; $^{***}P < 0.001$. ELISA, enzyme-linked immunosorbent assay; LNP, lipid nanoparticle; LPS, lipopolysaccharide; NS, not significant; siRNA, small interfering RNA; TNF-α, tumor necrosis factor-α.

correlation with the Western blot analysis, which revealed that PTEN protein levels were significantly reduced at distances within 1 mm of the injection tract but not 1–3 mm away (**Figure 5b**). To test the time course of PTEN knockdown following single injections of LNP-siRNA, the amount of PTEN protein expressed within 0.5 mm of the injection sites was measured using Western blots in a series of animals at different time points following injection. PTEN suppression following a single injection was sustained for at least 15 days (PTEN/β-actin reduced by 91% compared with control, $P < 0.001$, **Figure 5c**), the longest time point tested.

LNPs are capable of widespread distribution and knockdown after ICV administration

Although local knockdown can be quite useful when attempting to target specific brain regions, sometimes more widespread

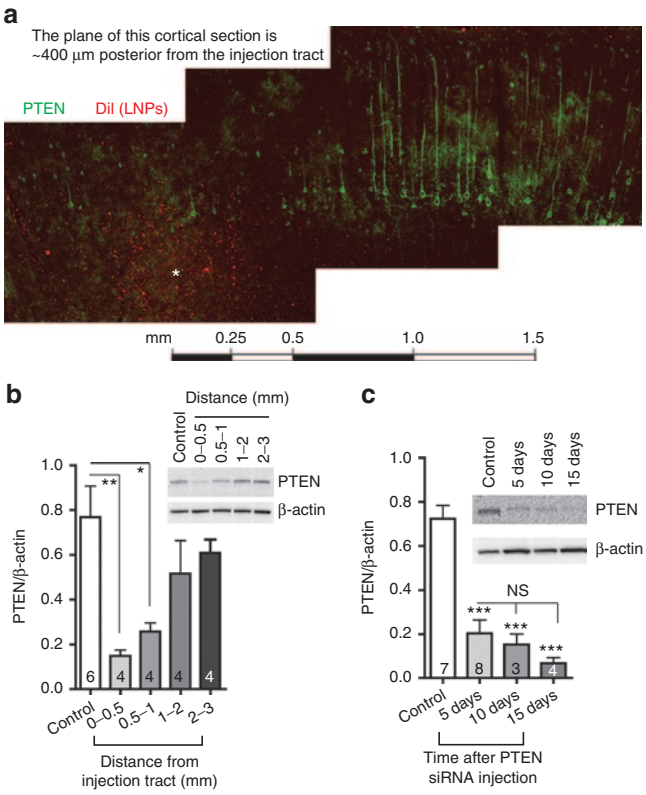

Figure 5 Distance profile and time course of protein knockdown *in vivo*. (**a**) Immunofluorescence for PTEN protein is decreased in neurons less than 1 mm from the site of LNP-siRNA injection. The illustrated montage was obtained from a section plane posterior to the injection tract and the asterisk indicates the point that was 400 μm from the injection. (**b**) An example Western blot (inset) shows decreased PTEN protein in tissue obtained less than 1 mm from the injection tract. Bar graph showing the summarized data from Western blots on tissue dissected at different distances adjacent to LNP-siRNA injection. (**c**) Western blot revealed sustained knockdown of PTEN at 5, 10, and 15 days following a single intracranial injection of LNP-siRNA. $^{*}P < 0.05$; $^{**}P < 0.01$; $^{***}P < 0.001$. LNP, lipid nanoparticle; NS, not significant; siRNA, small interfering RNA.

knockdown is preferable. We, therefore, tested whether intracerebroventricular (ICV) injections could overcome the distance limitations imposed by small volume local injections. For the purpose of this study, we focused on two brain regions close to the ventricular system, the dorsal hippocampus and the striatum. Following a single injection of 2 μl PTEN siRNA-LNPs bilaterally into the lateral ventricles, we observed robust LNP uptake in neurons as shown by DiI uptake in the CA1 cell body layer of the hippocampus (**Figure 6a**) at a distance over 4 mm from the injection site itself. We verified that the siRNA-LNP was effective by measuring PTEN levels in both the striatum and the dorsal hippocampus of rats injected with PTEN siRNA-LNPs (PTEN/β-actin reduced 55.8% in hippocampus and 51.2% in striatum compared with control siRNA–injected rats **Figure 6b–d**).

LNP-mediated knockdown of GluN1 in cell culture

The ability of LNP-siRNA technology to modify the synaptic function of nerve cells was tested. siRNA against

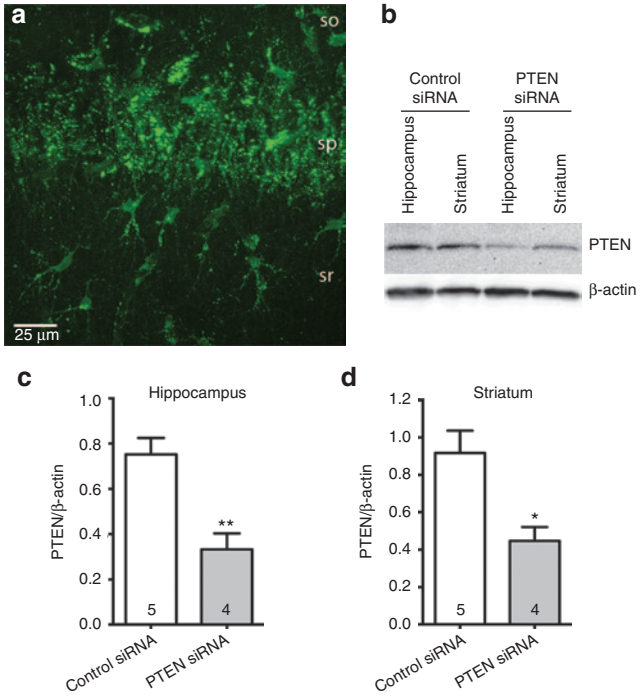

Figure 6 Lipid nanoparticles (LNPs) are capable of widespread distribution and knockdown after intracerebroventricular (ICV) administration. (**a**) DiI fluorescence in CA1 region of the hippocampus shows robust uptake of LNPs by neurons in the cell body layer (sp). Scale: 25 μm. (**b–d**) Western blots show ICV-injected siRNA-LNPs results in knockdown of the target protein (PTEN) in different brain regions (dorsal hippocampus and striatum). $^{*}P < 0.05$; $^{**}P < 0.01$. siRNA, small interfering RNA; so, stratum oriens; sp, stratum pyramidale (cell body layer); sr, stratum radiatum.

GRIN1, the gene encoding the GluN1 subunit of the NMDA receptor (NMDAR), was used to determine whether a LNP-siRNA delivery approach could effectively interfere with NMDAR function. The NMDAR ion channel is heteromeric, composed of two obligatory GluN1 subunits and two GluN2 or GluN3 subunits. Expression of GluN1 is necessary for the formation of a functional NMDAR channel in the plasma membrane.[19] Three different siRNAs directed against different regions of GRIN1 were tested using LNP delivery in cultured neurons to determine their efficacy. All three siRNA sequences resulted in significant knockdown of GluN1 expression (**Figure 7a**,**b**); however, sequence number 1 resulted in the most robust knockdown, and it was therefore used for the subsequent experiments *in vivo*. In addition, as a control for selectivity against the target gene, PTEN expression was not reduced by GluN1 siRNA (**Figure 7a**,**c**).

NMDARs are typically arranged in clusters at synaptic and extrasynaptic sites.[20,21] To test the effect of GluN1 knockdown on the presence of GluN1 clusters, cultures of cortical neurons were treated with LNPs containing either GluN1 siRNA or a control luc siRNA. Neurons exposed to LNP-GluN1 siRNA but not luc siRNA-LNP resulted in a significant decrease in the density of GluN1 clusters (GluN1 clusters/μm reduced by 41% compared with control, $P < 0.001$, **Figure 7d**,**e**).

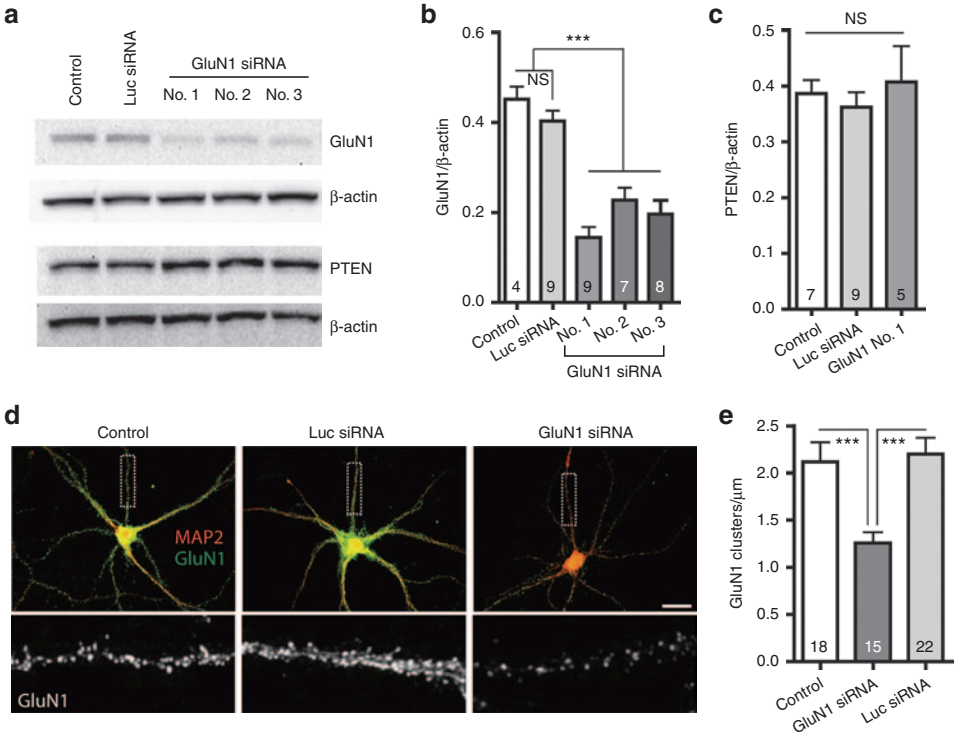

Figure 7 LNP-GluN1 siRNA results in knockdown of the NMDAR obligatory subunit GluN1. (**a**,**b**) Western blots show that LNP encapsulation of siRNAs targeted against three distinct regions of GluN1 RNA all resulted in knockdown of GluN1 protein (compared with nontreated control and luc siRNA). Mean knockdown with GluN1 siRNA no. 1 was greatest and was used for subsequent experiments. (**c**) Control shows LNP-GluN1 no. 1 siRNA did not affect PTEN expression. (**d**) Decreased GluN1 immunofluorescence was observed in LNP-GluN1 siRNA–treated cultures (right panels) as compared with nontreated (controls) or cultures treated with LNP-luc siRNA. Bottom: shows higher magnification of dashed box indicating GluN1 clusters along dendrite. Scale: 20 μm. (**e**) Summary data of GluN1 clusters/μm of dendrite. ***$P < 0.001$. LNP, lipid nanoparticle; NS, not significant; siRNA, small interfering RNA.

Functional knockdown of NMDAR currents *in vivo*

After establishing that LNP-encapsulated siRNA against GRIN1 can reduce GluN1 and therefore NMDAR expression *in vitro*, we proceeded to test the ability of this approach to knock down GluN1 expression and synaptic function *in vivo*. A single injection of LNPs containing GRIN1 siRNA resulted in a significant decrease in GluN1 protein expression compared with controls (no injection or rats injected with LNPs containing luc siRNA) when tested 5 days later (GluN1/β-actin reduced by 51 and 54% compared with noninjected and luc siRNA-LNP–injected controls, respectively, $P < 0.01$ and $P < 0.05$, **Figure 8a**,**b**). We then tested the functional impact of disrupting GluN1 expression by measuring the ratio of NMDAR/AMPA receptor (AMPAR) excitatory postsynaptic currents in voltage-clamped neurons. Glutamate is the major excitatory neurotransmitter in the brain and acts on both AMPAR and NMDAR at synapses. However, the NMDAR is normally blocked at resting membrane potential and requires the simultaneous binding of glutamate and depolarization to remove the voltage-dependent open channel block by extracellular Mg^{2+}. Therefore, a common protocol to test the NMDAR/AMPAR ratio in response to the synaptic release of glutamate is to measure the ratio of the evoked excitatory postsynaptic current when the NMDAR is blocked by holding the cell at –70 mV to obtain a pure AMPAR component versus when the cell is held at +40 mV to get a mixed AMPAR + NMDAR component (**Figure 8d**).[22,23]

Rats were injected with LNPs containing GluR1 siRNA or luc siRNA, and the NMDAR/AMPAR ratio was measured in cortical brain slices 4–6 days later, a time that corresponded to decreased expression of GluN1 expression as shown in Western blots. Neurons that were chosen for experiments were within 500 μm of the injection site and were verified to have taken up LNPs based on punctate intracellular DiI fluorescence (**Figure 8c**), and the ratio of NMDAR/AMPAR was measured. To get the NMDA component, we measured the amplitude of the outward current at V_h + 40 mV 50 ms after the stimulation artifact, a time point when the AMPAR current had returned to baseline (this was verified by subtracting the trace in the presence of the NMDAR antagonist, DL-2-amino-5-phosphonopentanoic acid (APV) to show the outward I_{NMDAR} (blue) and I_{AMPAR} (red) components separately). The AMPA component was measured as the inward current when the cell was held at –70 mV (**Figure 8d**). Consistent with the observed decrease in GluN1 expression, we found that neurons treated with LNPs that contained GluN1 siRNA had significantly decreased NMDAR/AMPAR ratios compared with neurons with LNPs from luc siRNA–injected rats (**Figure 8d–f**). Therefore, the NMDAR component of the synaptic response was selectively reduced by LNP-delivered GluN1 siRNA. These results further validate the use of LNPs to manipulate gene expression in the brain, showing that both the total protein levels and the function of the target protein were successfully disrupted.

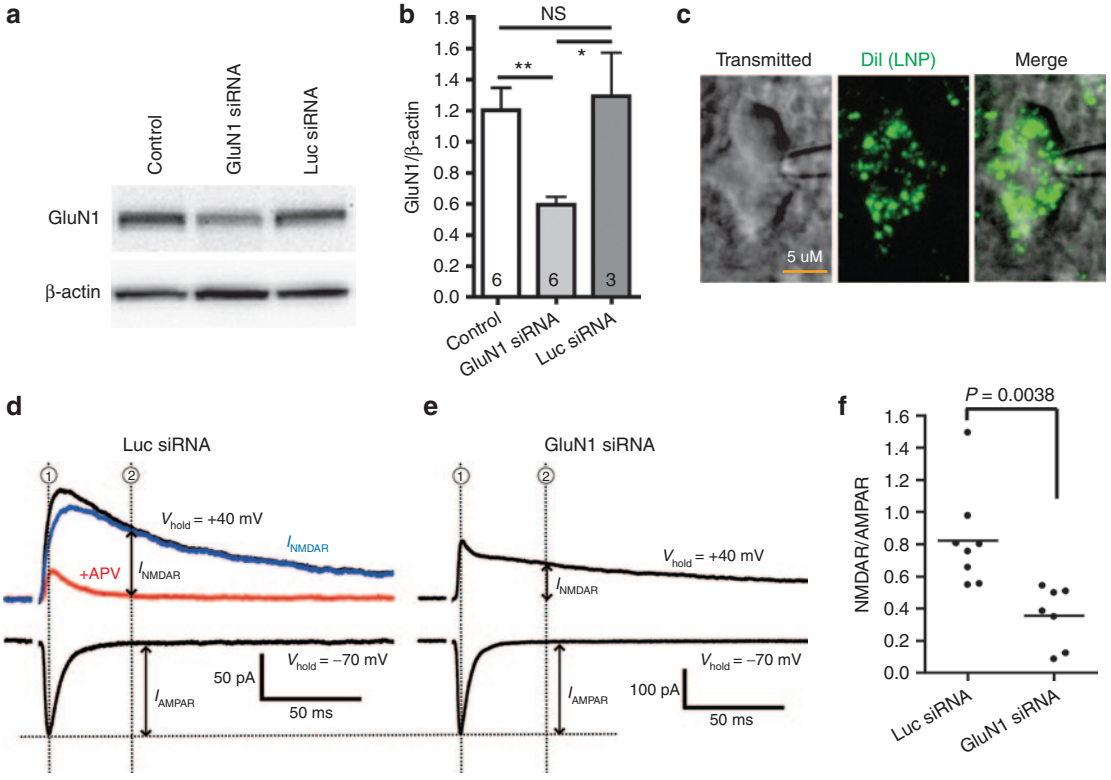

Figure 8 Selective knockdown of GluN1 protein *in vivo* results in functional disruption of NMDAR synaptic currents. (**a**,**b**) Western blot shows intracranial injection of LNP-GluN1 siRNA resulted in knockdown of GluN1 protein. Luc siRNA-LNP control injection showed no effect. (**c**) DiI staining was observed in a voltage-clamped neuron in a brain slice obtained 5 days after *in vivo* LNP injection indicating LNP uptake in this cell. (**d**) NMDA receptor (NMDAR)/AMPA receptor (AMPAR) ratio was calculated using the ratio of the NMDAR current at V_{hold} = +40 mV (upper traces) at point 2 when the AMPAR component (in the lower trace) returned to baseline (50 ms) divided by the peak current at V_{hold} = –70 mV (lower traces) at point 1 which was the peak AMPAR current. Red trace: in the presence of the NMDAR antagonist, APV, the NMDAR-dependent current was blocked revealing the outward AMPAR current. Blue trace: total current–red (APV) current = NMDAR component. (**e**,**f**) Voltage clamp revealed a selective decrease in NMDAR/AMPAR currents in neurons from rats injected with LNP-GluN1 siRNA compared with a luc siRNA-LNP control. *$P < 0.05$; **$P < 0.01$. LNP, lipid nanoparticle; NS, not significant; siRNA, small interfering RNA.

Discussion

The results presented in this article show that LNP-siRNA systems can exhibit efficient gene silencing properties in neurons both *in vitro* and *in vivo* that lead to functional consequences without inducing significant toxicity. In cell culture, 100% of neurons were observed to have taken up the LNPs as indicated by the appearance of DiI within the cytoplasm with no apparent toxicity or indications of neuron loss over several days to a week. In addition, the reduction of protein expression from siRNA was extensive enough to detect by Western blots using total protein from cultures or immunocytochemistry of individual neurons. In experiments *in vivo*, localized injection of siRNA-LNPs within the cortex or ICV injections to cause more diffuse and widespread LNP uptake led to consistent decreases in both mRNA and protein expression again with no indication of cell loss or damage from the uptake of LNPs.

In this article, we discuss the mechanism of action of LNP-siRNA delivery; the use of these LNP-siRNA systems for gene knockdown both *in vitro* and *in vivo* in the brain; and potential therapeutic applications with regard to neurological and psychiatric diseases. With respect to the mechanism of action, the LNP delivery systems used here contain the ionizable cationic lipid DMAP-BLP, a lipid that exhibits optimized bilayer destabilizing and pKa properties leading to highly potent gene silencing in hepatocytes following IV administration (**Supplementary Data**) that is similar to "gold standard" lipids such as DLinMC3-DMA.[8] Detailed studies have shown that the ability of LNP-siRNA systems containing related ionizable cationic lipids to induce hepatocyte gene knockdown *in vivo* is ApoE dependent.[10] In ApoE knockout mice, LNP-siRNA gene silencing activity is inhibited in hepatocytes and can be reestablished by incubating the LNPs with ApoE before IV administration. In the brain and neuronal cultures, ApoE is synthesized in astrocytes.[14,15] The astrocytes in the neuronal culture system are separated into a feeder layer that allowed us to test the ApoE dependence of LNP uptake by removing the separate astrocyte feeder layer. With no added ApoE, there was no evidence of neuronal LNP uptake, whereas graded uptake was observed when ApoE concentrations were increased above 0.1 μg/ml to 1 μg/ml and 5 μg/ml ApoE. The concentrations of ApoE found in the brain are similar to the concentrations we found to be effective in cell culture.[16] This suggests that the natural affinity of these LNP systems for endogenous ApoE in the brain provides a highly efficient method for LNP delivery into neurons *in vivo*.

The use of the LNP-siRNA systems for silencing target genes in neurons in cell culture is indicated by our observations

that transfection efficiencies approached 100%, without overt signs of toxicity. By contrast, current nonviral vectors exhibit transfection efficiencies of 10% or less and are often accompanied by cell damage.[13] LNPs appear to be a superior alternative to presently used techniques to transfect neurons in cell culture based not only on the high rate of uptake but also on the benign nature of the LNPs. Another key finding in our study is that the LNP-siRNA approach we describe here provides an effective alternative to other *in vivo* transfection vectors presently used. Viral delivery is the most effective available way to transfect neurons.[13,24] The disadvantage of viral delivery is the requirement for constructing virus vectors that take added time, potentially cause immune responses, and raise safety concerns. The use of LNPs can circumvent these issues, and provides a method to rapidly test various siRNA constructs against the expression of different target proteins, and then examine the protein's function. Injection of ASOs into the CSF represents another promising method to silence neuronal gene expression *in vivo*.[25] However, two major problems associated with ASOs are the high doses required to achieve gene silencing effects and immunostimulatory effects.[26,27] With regard to dose levels, ICV infusion of free ASOs against superoxide dismutase by osmotic pump at 100 μg/day per rat over 28 days (total of 2.8 mg of ASO) resulted in ~50% superoxide dismutase mRNA silencing.[28] In this article, we demonstrate that a single LNP-siRNA injection of 2.5 μg of siRNA per rat by intracortical administration results in pronounced (up to 91%) gene silencing that is sustained for at least 15 days after injection. Clinical studies suggest that the immunostimulatory effects of LNP-siRNA injections are infrequent and readily managed, see http://www.alnylam.com/capella/wp-content/uploads/2012/07/Alnylam-ALN-TTR02-PhaseI-Results-120716.pdf. Consistently, we found no evidence that LNP-siRNAs caused immunostimulatory effects in brain tissue as we found no increased synthesis of TNF-α triggered by LNPs (**Figure 4f**). In addition, there are now well-established methods to reduce or eliminate siRNA immunogenicity by adjusting siRNA chemistry.[29]

The LNP formulation employed here used PEG-DMG, which is a type of PEG-lipid with short acyl chains that allow it to dissociate rapidly[30] from LNPs upon dilution, allowing association of proteins such as ApoE. It would be expected that larger radii of distribution could be achieved for LNPs containing a PEG-lipid with longer acyl chains, which do not dissociate so rapidly. Enhanced tissue penetration would also be expected for smaller LNPs that can be achieved at higher PEG-lipid levels.[8] The LNP platform is highly flexible, potentially allowing delivery of other materials to neurons such as drugs, fluorescent dyes and plasmids.

The results presented in this article demonstrate the utility of LNP-siRNA systems for silencing target genes in neurons both *in vitro* and *in vivo*, with obvious utility for rapidly advancing functional genomics studies. The ability to silence multiple genes, even five or more genes at once,[31] may also prove useful. The therapeutic utility of direct intracranial administration of LNP-siRNA for treatment of neurological disorders remains to be established; however, there are now a number of clinically accepted therapies relying on direct pumping of therapeutics into the CSF.[32,33] A lipid-based formulation of cytarabine has gained clinical acceptance for treatment of brain cancer following direct administration into CSF.[34] Furthermore, a number of clinical trials are now in progress for treatments of serious neurological diseases that rely on continuous infusion of ASOs into the CSF.[27,28]

Materials and methods

LNP formulation and siRNA encapsulation. The ionizable cationic lipid DMAP-BLP and PEG lipid PEG-DMG were synthesized as described (**Supplementary Methods**). 1,2-distearoyl-sn-glycero-3-phosphocholine (DSPC) and cholesterol were obtained from Avanti (Alabaster, AL) and Sigma-Aldrich (St. Louis, MO), respectively. Lipophilic carbocyanine dyes to monitor LNP-siRNA uptake, 3,3′-dioctadecyloxacarbocyanine perchlorate ($DiOC_{18}$) and 1,1′-dioctadecyl-3,3,3′,3′-tetramethylindocarbocyanine perchlorate ($DiIC_{18}$), were obtained from Invitrogen (Carlsbad, CA). All lipid stocks were dissolved and maintained in 100% ethanol. Lipids were mixed together at a molar percentage ratio of 50% cationic lipid, 1.5% PEG-DMG, 37.5% cholesterol, 10% DSPC, and 1% $DiOC_{18}$ or $DiIC_{18}$. LNPs were prepared by mixing appropriate volumes of lipid stock solutions in ethanol with an aqueous phase containing siRNA duplexes using a microfluidic micromixer[7] provided by Precision NanoSystems (Vancouver, BC). For the encapsulation of siRNA, the desired amount of siRNA (0.056 mg siRNA: micromole of lipid) was dissolved in formulation buffer (25 mmol/l sodium acetate, pH 4.0). 1 × volume of the lipid in ethanol and 3 × volumes of the siRNA in formulation buffer were combined in the microfluidic micromixer using a dual-syringe pump (Model S200, KD Scientific, Holliston, MA) to drive the solutions through the micromixer at a combined flow rate of 2 ml/minute (0.5 ml/minute for syringe with lipid mixture and 1.5 ml/minute for syringe with siRNA in formulation buffer). The LNP-siRNA systems formed were then dialyzed for 4 hours against 50 mmol/l 2-(*N*-morpholino)ethanesulfonic acid (MES)/50 mmol/l sodium citrate buffer pH 6.7 followed by an overnight dialysis against 1× phosphate-buffered saline (PBS), pH 7.4 (GIBCO, Carlsbad, CA) using Spectro/Por dialysis membranes (molecular weight cutoff 12,000–14,000 Da, Spectrum Laboratories, Rancho Dominguez, CA). The mean diameter and polydispersity of the LNPs are listed in **Supplementary Table S1**. The size of LNPs was determined by dynamic light scattering (number mode; NICOMP 370 Submicron Particle Sizer, Santa Barbara, CA). Encapsulation efficiency was determined by quantifying siRNA by measuring absorbance at 260 nm in samples collected before and after dialysis following removal of free siRNA using VivaPureD MiniH columns (Sartorius Stedim Biotech, Aubagne, France). Lipid concentration was determined by measurement of cholesterol content by using a Cholesterol E enzymatic assay (Wako Chemicals USA, Richmond, VA). The final siRNA:lipid ratios (mg/μmol) are listed in **Supplementary Table S1**; g/l to moles/l conversions listed in **Supplementary Table S2**.

Hippocampal neuronal cultures and LNP treatments. Hippocampal cultures were prepared as described previously with a slight modification from that described in ref. 11. In brief, hippocampi were dissociated from 18-day-old rat embryos by treating with trypsin and then triturated with a constricted Pasteur pipette. Subsequently, the dissociated cells were plated on

poly-L-lysine–coated glass coverslip using minimum essential medium supplemented with 10% horse serum. Then, the coverslips were inverted over a feeder layer of astroglia cells to facilitate communication between neurons and feeder layer cells. Neurons were maintained in Neurobasal medium with B-27 and L-glutamine (Invitrogen). Cytosine arabinoside (5 μM; Calbiochem, Darmstudt, Germany) was treated after 2 days *in vitro* (DIV) to inhibit the proliferation of glia. Neuronal cultures were used for the experiment between days 12 and 14 in DIV. Cells were treated with LNPs (PTEN siRNA or luc siRNA) or with PTEN siRNAs without encapsulation.

Intracranial and ICV injections. All experimental protocols were approved by the Committee on Animal Care, University of British Columbia and conducted in compliance with guidelines provided by the Canadian Council of Animal Care. Sprague–Dawley rats (P22-P26) were anesthetized with isofluorane before and throughout the surgery. A small hole (diameter ~1 mm) was drilled in the skull to allow access to the brain (–2.0 mm anterior/posterior (AP) and ±3.0 mm medial/lateral (ML) from bregma and 0.8 mm dorsal/ventral (DV)). A glass micropipette (tip diameter ~40 μm) was connected to a Hamilton syringe and injected using an infusion pump (Harvard Apparatus, Holliston, MA) at a rate of 50 nl/minute. The total volume injected was 500 nl of LNP-siRNA (5 mg siRNA/ml in sterile PBS). For ICV injections, holes were drilled—0.8 mm AP and ±1.4 mm ML from bregma and –3.1 mm DV—and microdialysis silicon tubing was used to inject LNPs. The total volume injected was 2 μl bilaterally at a rate of 200 nl/minute.

Brain slice preparation. Five days after LNP-siRNAs (GluN1, PTEN, and luciferase) were injected into the cortex, Sprague–Dawley rats (postnatal day 26–30) were anesthetized with halothane and decapitated according to protocols approved by the University of British Columbia Committee on Animal Care. Brains were rapidly extracted and placed into ice-cold slicing solution containing (in mmol/l): NMDG, 120; KCl, 2.5; $NaHCO_3$, 25; $CaCl_2$, 1; $MgCl_2$, 7; NaH_2PO_4, 1.25; glucose, 20; Na-pyruvate, 2.4; and Na-ascorbate, 1.3; saturated with 95% O_2/5% CO_2. Coronal hemisections, 300 μm thick, were sliced using a vibrating tissue slicer (VT1200, Leica, Nussloch, Germany). For Western blot preparation, tissue within 1 mm but not including the injection sites (needle tracts) was collected. For electrophysiology experiments, slices were incubated at 32 °C in artificial CSF containing (in mmol/l): NaCl, 126; KCl, 2.5; $NaHCO_3$, 26; $CaCl_2$, 2.0; $MgCl_2$, 1.5; NaH_2PO_4, 1.25; and glucose, 10; saturated with 95% O_2/5% CO_2 for 45 minutes. For experiments, slices were at 22–24 °C and perfused at ~2 ml/minute.

Electrophysiology. Whole-cell patch clamp recordings were made using electrodes (4–6 MΩ resistance) filled with a pipette solution containing (in mmol/l): Cs-methanesulfonate, 108; Na-Gluconate, 8; Cs-EGTA, 1; TEA-Cl, 8; $MgCl_2$, 2; HEPES, 10; K_2ATP, 4; and Na_3GTP, 3; at pH 7.2. Whole-cell voltage-clamp recordings were obtained from neurons of the somatosensory cortex (layer 5) under microscope guidance using infrared differential interference contrast microscopy. All recordings were filtered at 2 kHz, digitized at 10 kHz, and acquired with Clampex (Axon Instruments, Foser City, CA). Membrane potential was clamped at –70 mV. A monopolar stimulation electrode was positioned at ~100 μm from the soma of the recorded neuron. The extracellular solutions were supplemented with 50 μmol/l picrotoxin (Sigma) and 8 mmol/l of each $MgCl_2$ and $CaCl_2$ to block $GABA_A$ synaptic potentials, block epileptiform activity, and minimize polysynaptic responses. Synaptic responses were evoked with monophasic voltage pulses every 10 seconds. Cells were allowed to dialyze for at least 15 minutes before starting recordings. Access resistance was continuously monitored during the experiments. The AMPAR excitatory postsynaptic current was recorded at V_{hold} = –70 mV followed by the NMDAR + AMPAR excitatory postsynaptic current at V_{hold} = +40 mV. V_{hold} was then returned to –70 mV at the end of the experiment to verify that there was no change in the baseline. Twenty to fifty traces were averaged per recording. A 25 μmol/l D-APV (Abcam Biochemicals, Cambridge, MA) was applied to some experiments to illustrate outward NMDAR and AMPA currents. Signals were amplified with the Multiclamp 700B amplifier (Axon Instruments), low-pass filtered at 2 kHz, and digitized at 10 kHz using the Digidata 1322 (Axon Instruments). Data were collected (pClamp, version 9.2; Axon Instruments) and stored on computer for offline analysis using clampfit software (Axon Instruments).

Imaging. Live cell imaging (brain slice) was performed with a two-photon laser-scanning microscope (Zeiss LSM510-Axioskop-2; Zeiss, Oberkochen, Germany) with a 40X-W/1.0 numerical aperture objective lens directly coupled to a Chameleon ultra2 laser (Coherent, Santa Clara, CA). DiI and CoroNa were excited at 760 nm, the fluorescence from each fluorophore was split using a dichroic mirror at 560 nm, and the signals were each detected with a dedicated photo multiplier tube after passing through an appropriate emission filter (DiI: 605 nm, 55 nm band pass; CoroNa: 525 nm, 50 nm band pass). Transmitted light was simultaneously collected using understage infrared differential interference contrast optics and an additional photo multiplier tube. For AM dye loading, slices were incubated at 32 °C for 45 minutes at 16.7 μg/ml. Cell density was measured in 10 μm *z*-stacks of 200×200 μm, and all cells including partial cells were counted, therefore resulting in an overestimate of cell density/mm^3.

Immunohistochemistry. Free-floating sections (40 μm transverse sections) were processed for immunostaining as described previously.[35] The primary antibodies used for immunostaining were as follows: rabbit anti-PTEN (Santa Cruz, Dallas, TX, 1:300), mouse antimicrotubule associated protein-2 (MAP-2; Chemicon, Temecula, CA, 1:2,000). Alexa Fluor 633 antimouse or Alexa Fluor 488 antirabbit IgG (1:1,000) secondary antibodies (Invitrogen) were used for immunofluorescent staining. As a negative control experiment, primary antibody was omitted during the immunostaining.

Immunocytochemistry. Rat hippocampal neurons (DIV 12–14 days) grown on poly-L-lysine–coated glass coverslips were incubated in neurobasal media with LNP-siRNAs (luciferase siRNA and GluN1 siRNA) for 48 hours and then processed with immunostaining. In brief, cells were fixed in 2% paraformaldehyde in 0.1 M PBS for 10 minutes, washed with PBS, and then permeabilized in 0.05% Tween20 in 0.1 M PBS for 20 minutes. Cells were then incubated in mouse anti-GluN1 (1:300

dilution; Invitrogen) or rabbit anti-MAP-2 at 4 °C for 24 hours and followed by Alexa Fluor 488 antimouse IgG secondary antibody (1:1,000; Molecular Probes, Eugene, OR) or Alexa Fluor 633 antirabbit IgG (1:1,000) incubation at room temperature for 1 hour in the dark. After PBS washes, coverslips were then immersed in 4′,6-diamidino-2-phenylindole (DAPI; Molecular Probes) at 1 μg/ml in water to visualize cell nuclei. The coverslips were mounted onto glass slides using Fluoro-Save (Calbiochem) and examined under an Olympus confocal microscope (FluoView 1000, Olympus, Center Valley, PA).

Western blotting. Cultured rat hippocampal neurons and rat cortical brain slices were used for Western blotting. At 5 days after injection with LNP-siRNAs (GluN1, PTEN, and luciferase) into the cortex, cortical brain slices were prepared as previously described.[35] Cells and brain slices were homogenized using lysis buffer containing (in mmol/l): Tris pH 7.0, 100; EGTA, 2; EDTA, 5; NaF, 30; sodium pyrophosphate, 20; 0.5% NP40 with phosphatase, and protease inhibitor cocktail (Roche, Basel, Switzerland). The homogenates were then centrifuged at 13,000*g* (20 minutes, 4 °C) to remove cellular debris, then protein concentrations of the crude lysates were determined by performing a Bradford assay with the DC Protein Assay dye (Bio-Rad, Mississauga, Ontario, Canada). The protein samples were diluted with 2× Laemmli sample buffer and boiled for 5 minutes. Following sodium dodecyl sulfate/polyacrylamide gel electrophoresis, proteins were transferred to polyvinylidene fluoride membranes, blocked in 5% milk overnight at 4 °C, rinsed with Tris-buffered saline with 0.1% Tween 20 (TBST), and incubated with mouse anti-GluN1 monoclonal antibody (1:300) or rabbit anti-PTEN polyclonal antibody (1:300) overnight at 4 °C. Following four washes with TBST, the membranes were incubated with the antimouse or antirabbit secondary antibody conjugated to horseradish peroxidase (1:500) for 1 hour at room temperature. The membranes were then washed 3–4 times (15 minutes) with TBST, and bands were visualized using enhanced chemiluminescence (GE HealthCare, Cleveland, OH).

Tissue analyzed from ICV injections was sampled as follows. Entire dorsal hippocampal slices were dissected from –2.0 to –4.2 mm AP from bregma. Striatal slices were taken from +1.0 to –0.5 mm AP from bregma within 1.5 mm from the ventricle border.

LDH assay. LDH assay kits (Biomedical Research Service Center, State University of New York at Buffalo) were used to examine cell death using cultures of hippocampal neurons with astrocytes on a separate feeder layer. Cells were treated with LNP-siRNA (luciferase siRNA) for 72 hours then assessed for cell death using LDH assay. Media containing Triton X-100 (1%) was used as a positive control for cell death. Supernatants were collected at 72 hours after the treatment, and then cells on the coverslips were lysed using lysis buffer. The LDH level in the supernatant represents the cell death, whereas the LDH level in lysed cells represents the viable cells. In brief, supernatants and cell lysates were centrifuged for 3 minutes at maximal speed (16,000*g*) at 4 °C. All samples were added into a 96-well plate with LDH assay solution and incubated for 30 minutes at 37 °C. The reaction was stopped with 3% acetic acid. LDH reduces tetrazolium salt INT to formazan, which is water soluble and exhibits an absorption maximum at 492 nm. Absorbance at 492 nm was measured using a microplate reader. Cell death was calculated as percentage of released LDH compared with the sum of superfusate LDH and cell lysate LDH.

DiI uptake assay. Cortical neuronal cultures (3×10^4 cells in 12-well plate) were treated with luc siRNA-LNP (at 1.6 μg/ml) conjugated with DiI for 2 hr in the absence and presence of recombinant ApoE4 (Peprotech, Rocky Hill, NJ) at different concentrations (0.1, 1, 5, 10 μg/ml). Then, cultures were washed five times with PBS to wash out unbound luc siRNA-LNP. Subsequently, 400 μl of filtered dH_20 was added to the wells to rupture cells. DiI fluorescence was measured (excitation at 520 nm, emission at 578 nm) using Gemini fluorescence microplate reader systems (Molecular Devices Corporation, Union city, CA). Fluorescence reading from the untreated group was subtracted from other groups.

TNF-α ELISA. ELISAs were performed according to the manufacturer instructions (eBioscience, San Diego, CA). In brief, hippocampal brain slices (400 μm) were incubated and treated in a homemade chamber (using six multiwell plates) equipped with continuous aeration with 95% O_2/5% CO_2. Slices were treated with luc siRNA-LNPs (3.3 μg/ml) for 5 hours. As a positive control, lipopolysaccharide (40 μg/ml) was treated to the slices. Then, the hippocampal brain slices were harvested and homogenized. Cell lysates were centrifuged for 20 minutes at 4 °C, and subsequent supernatants were used for protein assay and TNF-α measurement.

siRNA sequences and chemistry. PTEN siRNA: the PTEN siRNA strands had the following sequence and chemistry: sense strand, 5′-GAuGAuGuuuGAAAcuAuudTsdT-3′ and antisense strand 5′-AAuAGUUUcAAAcAUcAUCdTsdT-3′ where the uppercase letters represent unmodified ribonucleotides, lowercase letters represent 2′-OMe modified nucleotides, and "s" represents a phosphorothioate (P=S) linkage between the two dT at the 3′-end. The P=S linkage provided protection from exonuclease degradation, and the 2′-OMe modifications reduced potential for immunostimulatory activity and provided stability toward endonucleolytic degradation.

Luciferase siRNA had the following sequence as previously described:[36] sense strand, 5′- cuuAcGcuGAGuA cuucGAdTsdT-3′

- and antisense strand, 5′-UCGAAGuACUcAG CGuAAGdTsdT-3′ with the modification designation as listed above.

GRIN1 siRNA: the sequences of "stealth siRNA" (Invitrogen Life Technologies, Gaithesburg, MD) had the following sequences: GRIN1 no. 1, sense strand, 5′-UGCAU GUCCCAUCACUCAUUGUGGG-3′ and antisense strand, 5′-CCCACAAUGAGUGAUGGGACAUGCA-3′; GRIN1 no. 2, sense strand, 5′-CUUCUGUGAAGCCUCAAACUCCAGC-3′ and antisense strand, 5′-GCUGGAGUUUGAGGCUUCACA GAAG-3′; GRIN1 no. 3, sense strand, 5′-UUGACGUACACG AAGGGCUCUUGGU-3′ and antisense strand, 5′-ACCAA GAGCCCUUCGUGUACGUCAA-3′.

The reason for variations in the siRNA constructs is due to production from different suppliers.

Statistical analysis. Experimental values are presented as mean ± SEM, expressed in percent from 100% baseline. The "*n*" value represents the number of experiments conducted for analysis. Statistical analyses were performed using a two-tailed Student's *t*-test or ANOVA followed by Newman–Keuls multiple comparison test. $P < 0.05$ was accepted as statistically significant ($^{*}P < 0.05$; $^{**}P < 0.01$; $^{***}P < 0.001$).

Supplementary material

Table S1. LNP-siRNA properties.
Table S2. Conversion table for siRNA concentrations.
Supplementary Methods.

Acknowledgments. P.R.C. acknowledges funding from the Canadian Institutes of Health Research (CIHR) Funding reference number 111627. B.A.M. was funded by CIHR (Funding reference numbers 244825 and 245760), Fondation Leducq, Human Frontiers Science Program, and the MIRI Program from Brain Canada. R.L.R. and R.W.Y.K. have studentships from CIHR. The authors thank Alnylam Pharmaceuticals for providing the lipids DMAP-BLP and PEG-DMG and Precision NanoSystems for the microfluidic mixing apparatus. They also thank Barbara L Mui and Ying K Tam (AlCana Technologies) for conducting the pKa and FVII gene silencing studies on LNP containing DMAP-BLP as indicated in **Supplementary Data**. The authors thank Xiling Zhou and Anne Marie Craig for supplying neuronal cultures and Kate Campbell for illustrations. P.R.C. is a shareholder of Alnylam Pharmaceuticals and a founder and shareholder of Precision NanoSystems. B.A.M. is a shareholder of Precision NanoSystems. Alnylam supports research in the PRC laboratory through a sponsored research agreement. J.N. and M.M. are employees of Alnylam. R.L.R, H.B.C., P.J.C.L., R.W.Y.K, and D.A. have no potential conflicts of interest.

1. Fire, A, Xu, S, Montgomery, MK, Kostas, SA, Driver, SE and Mello, CC (1998). Potent and specific genetic interference by double-stranded RNA in Caenorhabditis elegans. *Nature* **391**: 806–811.
2. Sun, HS, Jackson, MF, Martin, LJ, Jansen, K, Teves, L, Cui, H *et al.* (2009). Suppression of hippocampal TRPM7 protein prevents delayed neuronal death in brain ischemia. *Nat Neurosci* **12**: 1300–1307.
3. Zimmermann, TS, Lee, AC, Akinc, A, Bramlage, B, Bumcrot, D, Fedoruk, MN *et al.* (2006). RNAi-mediated gene silencing in non-human primates. *Nature* **441**: 111–114.
4. Davidson, BL and McCray, PB Jr (2011). Current prospects for RNA interference-based therapies. *Nat Rev Genet* **12**: 329–340.
5. Semple, SC, Akinc, A, Chen, J, Sandhu, AP, Mui, BL, Cho, CK *et al.* (2010). Rational design of cationic lipids for siRNA delivery. *Nat Biotechnol* **28**: 172–176.
6. Basha, G, Novobrantseva, TI, Rosin, N, Tam, YY, Hafez, IM, Wong, MK *et al.* (2011). Influence of cationic lipid composition on gene silencing properties of lipid nanoparticle formulations of siRNA in antigen-presenting cells. *Mol Ther* **19**: 2186–2200.
7. Lee, JB, Zhang, K, Tam, YY, Tam, YK, Belliveau, NM, Sung, VY *et al.* (2012). Lipid nanoparticle siRNA systems for silencing the androgen receptor in human prostate cancer in vivo. *Int J Cancer* **131**: E781–E790.
8. Belliveau, NM, Huft, J, Lin, PJ, Chen, S, Leung, AK, Leaver, TJ *et al.* (2012). Microfluidic synthesis of highly potent limit-size lipid nanoparticles for *in vivo* delivery of siRNA. *Mol Ther Nucleic Acids* **1**: e37.
9. Jayaraman, M, Ansell, SM, Mui, BL, Tam, YK, Chen, J, Du, X *et al.* (2012). Maximizing the potency of siRNA lipid nanoparticles for hepatic gene silencing in vivo. *Angew Chem Int Ed Engl* **51**: 8529–8533.
10. Akinc, A, Querbes, W, De, S, Qin, J, Frank-Kamenetsky, M, Jayaprakash, KN *et al.* (2010). Targeted delivery of RNAi therapeutics with endogenous and exogenous ligand-based mechanisms. *Mol Ther* **18**: 1357–1364.
11. Craig, AM, Banker, G, Chang, W, McGrath, ME and Serpinskaya, AS (1996). Clustering of gephyrin at GABAergic but not glutamatergic synapses in cultured rat hippocampal neurons. *J Neurosci* **16**: 3166–3177.
12. Kwon, CH, Luikart, BW, Powell, CM, Zhou, J, Matheny, SA, Zhang, W *et al.* (2006). Pten regulates neuronal arborization and social interaction in mice. *Neuron* **50**: 377–388.
13. Karra, D and Dahm, R (2010). Transfection techniques for neuronal cells. *J Neurosci* **30**: 6171–6177.
14. Pitas, RE, Boyles, JK, Lee, SH, Foss, D and Mahley, RW (1987). Astrocytes synthesize apolipoprotein E and metabolize apolipoprotein E-containing lipoproteins. *Biochim Biophys Acta* **917**: 148–161.
15. Bu, G (2009). Apolipoprotein E and its receptors in Alzheimer's disease: pathways, pathogenesis and therapy. *Nat Rev Neurosci* **10**: 333–344.
16. Wahrle, SE, Shah, AR, Fagan, AM, Smemo, S, Kauwe, JS, Grupe, A *et al.* (2007). Apolipoprotein E levels in cerebrospinal fluid and the effects of ABCA1 polymorphisms. *Mol Neurodegener* **2**: 7.
17. Thorne, RG and Nicholson, C (2006). *In vivo* diffusion analysis with quantum dots and dextrans predicts the width of brain extracellular space. *Proc Natl Acad Sci USA* **103**: 5567–5572.
18. Tsien, RY (1981). A non-disruptive technique for loading calcium buffers and indicators into cells. *Nature* **290**: 527–528.
19. Traynelis, SF, Wollmuth, LP, McBain, CJ, Menniti, FS, Vance, KM, Ogden, KK *et al.* (2010). Glutamate receptor ion channels: structure, regulation, and function. *Pharmacol Rev* **62**: 405–496.
20. Rao, A and Craig, AM (1997). Activity regulates the synaptic localization of the NMDA receptor in hippocampal neurons. *Neuron* **19**: 801–812.
21. Washbourne, P, Bennett, JE and McAllister, AK (2002). Rapid recruitment of NMDA receptor transport packets to nascent synapses. *Nat Neurosci* **5**: 751–759.
22. Sah, P and Nicoll, RA (1991). Mechanisms underlying potentiation of synaptic transmission in rat anterior cingulate cortex *in vitro*. *J Physiol (Lond)* **433**: 615–630.
23. Mameli, M, Bellone, C, Brown, MT and Lüscher, C (2011). Cocaine inverts rules for synaptic plasticity of glutamate transmission in the ventral tegmental area. *Nat Neurosci* **14**: 414–416.
24. Hommel, JD, Sears, RM, Georgescu, D, Simmons, DL and DiLeone, RJ (2003). Local gene knockdown in the brain using viral-mediated RNA interference. *Nat Med* **9**: 1539–1544.
25. Kordasiewicz, HB, Stanek, LM, Wancewicz, EV, Mazur, C, McAlonis, MM, Pytel, KA *et al.* (2012). Sustained therapeutic reversal of Huntington's disease by transient repression of huntingtin synthesis. *Neuron* **74**: 1031–1044.
26. Zalachoras, I, Evers, MM, van Roon-Mom, WM, Aartsma-Rus, AM and Meijer, OC (2011). Antisense-mediated RNA targeting: versatile and expedient genetic manipulation in the brain. *Front Mol Neurosci* **4**: 10.
27. Robinson, R (2012). Antisense therapy for ALS found safe, but more safety data are sought. *Neurol Today* **12**: 4–5.
28. Smith, RA, Miller, TM, Yamanaka, K, Monia, BP, Condon, TP, Hung, G *et al.* (2006). Antisense oligonucleotide therapy for neurodegenerative disease. *J Clin Invest* **116**: 2290–2296.
29. Bramsen, JB and Kjems, J (2012). Development of Therapeutic-Grade Small Interfering RNAs by Chemical Engineering. *Front Genet* **3**: 154.
30. Holland, JW, Hui, C, Cullis, PR and Madden, TD (1996). Poly(ethylene glycol)–lipid conjugates regulate the calcium-induced fusion of liposomes composed of phosphatidylethanolamine and phosphatidylserine. *Biochemistry* **35**: 2618–2624.
31. Love, KT, Mahon, KP, Levins, CG, Whitehead, KA, Querbes, W, Dorkin, JR *et al.* (2010). Lipid-like materials for low-dose, *in vivo* gene silencing. *Proc Natl Acad Sci USA* **107**: 1864–1869.
32. Dash, AK and Cudworth, GC 2nd (1998). Therapeutic applications of implantable drug delivery systems. *J Pharmacol Toxicol Methods* **40**: 1–12.
33. North, RB and Levy, RM (1997). *Neurosurgical Management of Pain*. Springer: New York, NY.
34. Phuphanich, S, Maria, B, Braeckman, R and Chamberlain, M (2007). A pharmacokinetic study of intra-CSF administered encapsulated cytarabine (DepoCyt) for the treatment of neoplastic meningitis in patients with leukemia, lymphoma, or solid tumors as part of a phase III study. *J Neurooncol* **81**: 201–208.
35. Choi, HB, Gordon, GR, Zhou, N, Tai, C, Rungta, RL, Martinez, J *et al.* (2012). Metabolic communication between astrocytes and neurons via bicarbonate-responsive soluble adenylyl cyclase. *Neuron* **75**: 1094–1104.
36. Addepalli, H, Meena, Peng, CG, Wang, G, Fan, Y, Charisse, K *et al.* (2010). Modulation of thermal stability can enhance the potency of siRNA. *Nucleic Acids Res* **38**: 7320–7331.

Supplementary Information accompanies this paper on the Molecular Therapy–Nucleic Acids website (http://www.nature.com/mtna)